Surface Science 223 (1989) 258–284
North-Holland, Amsterdam

LEED INVESTIGATION OF TEMPERATURE-DEPENDENT SURFACE ORDER OF Pb SINGLE CRYSTAL SURFACES

U. BREUER, H.P. BONZEL, K.C. PRINCE

Institut für Grenzflächenforschung und Vakuumphysik, Kernforschungsanlage Jülich GmbH, 5170 Jülich, Fed. Rep. of Germany

and

R. LIPOWSKY *

Institut für Festkörperforschung, Kernforschungsanlage Jülich GmbH, 5170 Jülich, Fed. Rep. of Germany

Received 28 April 1989; accepted for publication 26 July 1989

The intensities of several LEED beams from clean Pb(110) and Pb(111) surfaces have been measured in the temperature range from 200 to 590 K and 585 K, respectively. For Pb(111) the intensities show a normal Debye–Waller type decrease with increasing temperature up to 585 K, where LEED spots are still visible. For Pb(110), on the other hand, an additional intensity drop is seen at 490 K and above indicating an order–disorder phase transition. The intensity behavior for (10) and (01) beams of Pb(110) is distinctly different in the sense that disordering along the $[1\bar{1}0]$ direction is faster than along [001]. This anisotropy in disorder remains visible up to 590 K where the (01) beam still has residual intensity whereas the (10) beam is indistinguishable from the background. A quantitative evaluation suggests that the phase boundary in the $[1\bar{1}0]$ direction is atomically sharp while that in the [001] direction is fairly diffuse. The evaluation is carried out in terms of an anisotropic order parameter function.

1. Introduction

Melting of solids, metals in particular, has caught the fancy of scientists for many years. The question whether melting is initiated at the surface of a solid is one of the focal points of this long standing attention. Experiments with melting of small particles [1], thin films [2–5] and with bulk samples of Cu [6], Ga [7], Na [8], Pb [9–14] and Al [15] have produced results that favor a lower

---

* Present address: Sektion Physik der Universität München, Theresienstrasse 37, 8000 München 2, Fed. Rep. of Germany.

0039-6028/89/$03.50

"melting temperature" at the surface than the thermodynamically well-defined bulk melting temperature. However in two cases [16,17] the authors did not observe an effect that in their opinion supported surface melting below the bulk melting temperature. Thus there are two conflicting opinions in this interesting field which have led to controversial discussion. Such discussion has also occurred in the past [18,19] in the context of surface self-diffusion phenomena [20]. Clearly, the temperature dependence of surface self-diffusion of metals in the vicinity of the melting point ought to relate to the problem of surface melting if it exists. This point as well as a review of experimental and theoretical details of surface melting have been nicely summarized by Nenow [21] and more recently by van der Veen [22].

Another modern approach to the study of melting concentrates on Lennard-Jones-type solids, i.e. films of solid inert gases [23–25]. This work is related to the earlier experiments with deposited thin metal films [2,3] but its interpretation should be simpler because of the weaker interaction between film and substrate. Another related observation appears to be a phase transition at the Ge(111) surface at 150 K below the bulk melting point [26]. Although this phase transition is characterized by a loss in lateral crystalline order for the outermost layers, it is not clear whether this indicates "surface melting" [26].

The controversy, from an experimental point of view, is most obvious with Pb because two groups have reported no surface melting [16,17] whereas another group has published a series of papers with clear evidence of surface disordering some 20 degrees below the bulk melting temperature, T_m, for Pb(110) [9,10,14] and similar effects for vicinal Pb surfaces [11]. The results of this latter group were obtained by Rutherford backscattering (RBS) of H^+ ions. This technique probes predominantly the short-range order of a solid. If a complete loss of short-range order occurs about 20 K below T_m, a concomitant loss of long-range order must occur. However, a previous study of Pb(110) by low-energy electron diffraction (LEED) which probes specifically long-range order, showed apparently no effect [16] although no beam intensity versus temperature data were published.

The motivation for the present study of Pb(110) and Pb(111) by LEED derives from the apparent contradiction between the RBS and previous LEED results [9,10,16]. If for Pb(110) a complete loss of short-range order is observed near 580 K, with the thickness of the disordered layer growing to as much as 25 monolayers of Pb [9,10,14], it should be easy to detect this effect by LEED. First of all LEED is sensitive to long-range order, and secondly, it is surface-sensitive such that beam intensities should easily discriminate between order and disorder in one to three surface layers. Since according to Pluis et al. [11] the surface melting effect is largest for Pb(110) and absent for Pb(111), we decided to compare the LEED intensity versus temperature behavior for these two crystal orientations.

An obvious problem with studies of surface melting is the maintenance of absolute surface cleanliness. At temperatures near the melting point diffusion becomes rapid, and the enrichment of the surface region of the crystal by impurities is more likely than at low temperatures. Some impurities may be able to lower the bulk melting point of the material under investigation – a problem that has worried previous investigators [10,22]. We will therefore spend some time in describing the cleaning procedure of our Pb crystals and also the continuous control of surface purity by Auger electron spectroscopy (AES). We will then present intensity versus temperature traces of several LEED beams at various primary energies to illustrate the difference between Pb(111) and Pb(110) orientations, and to describe the loss of long-range order for Pb(110) below T_m. This process of disordering will be shown to be anisotropic in that the degree of order versus temperature for the $[1\bar{1}0]$ azimuth is lower than for the [001] azimuth, for all temperatures below 590 K. This anisotropy in disorder constitutes a difference between the surface melted (or premelted [10]) phase and the melt at T_m where disorder is totally isotropic.

2. Experimental

2.1. Sample heating and LEED

The sample heater and support was a thin copper plate (30×20 mm^2) which could be heated by a miniature sheathed heating element (Thermocoax, registered trademark of Philips GmbH) in the form of a loop pressed into a slotted plate for good thermal contact. The Pb crystal was held to the Cu plate by means of tantalum strips that were fitted into slots on both sides of the crystal. Good thermal contact between Cu plate and Pb crystal was assured by the flatness of both surfaces. The temperature of the crystal was measured by an iron–constantan thermocouple inserted into a hole in the crystal. The emf of the thermocouple was measured against a reference thermocouple at 273 K (ice water).

The sample could be cooled to about 200 K via a liquid nitrogen cold finger connected to the Cu plate by a braided Cu connection. Cooling of the crystal was advantageous for reducing the influence of the Debye–Waller factor in order to obtain good LEED patterns. LEED played an important role during the initial crystal cleaning period, in particular as an indicator of good crystalline order at the surface.

The Cu plate heater with integral wire loop exhibited a very small magnetic field during operation with a current of about 1.8 A. To circumvent any possible effects due to this field, the current was kept constant during a measurement. The beam (spot) position on the fluorescent screen remained

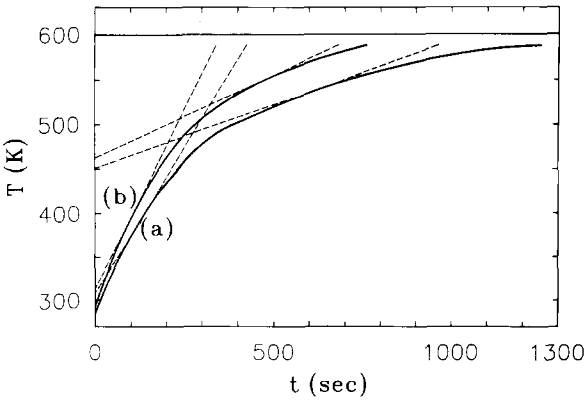

Fig. 1. Sample heating curve, $T(t)$. (a) Heating current 1.6 A. (b) Heating current 1.8 A. Dashed lines indicate temperatures at which the heating rate (gradient) was calculated. Values range from 0.8 to 0.1 K/s.

fixed such that a readjustment of the spot photometer was unnecessary. Heating was started at 200 K but the range 200–350 K was generally not used for evaluation. Fig. 1 shows a representative example of the crystal temperature versus time during such a measurement of $I(T)$. The heating rate varies between 0.8 K/s (maximum) and 0.1 K/s (minimum). These rates are low such that we can assume that the crystal is in thermal equilibrium at all times during the beam intensity measurement.

LEED was carried out with a standard 3-grid system (Physical Electronics). For Pb(110) all beams except (00) were visible on the screen at normal incidence. The (00) beam was visible at an angle of incidence of about 3°. At higher primary beam energy LEED was operated in the field-free mode but at low primary energies (< 19 eV) a negative bias of up to 18 V was placed on the crystal such that the diffracted beams could still be observed on the screen at normal incidence. For Pb(111) LEED beams other than (00) were only visible on the screen at an angle of incidence of about 7°, including low primary energies (< 19 eV) when a negative bias of about 24 V was placed on the crystal. The low primary beam energies were chosen to minimize the effect of the Debye–Waller factor. The relative intensity decrease due to surface disordering was particularly large under these conditions such that $I(T)$ measurements at the lowest achievable primary beam energies carry a large weight in this investigation.

The intensities of LEED beams were measured by a spot photometer focused onto the particular spot on the fluorescent screen. This photometer could be operated with a variable aperture between 2′ and 3°. The aperture of 6′ was generally sufficient to cover the entire spot and some area next to it. We did not observe spot broadening for all temperatures where the spot was still visible to the naked eye. Since measurements with a larger aperture of 12′ gave similar results we assume that all recorded changes in spot intensity are not influenced by spot profile changes. This assumption was checked in a later investigation by video LEED and no significant broadening was observed [27].

2.2. Sample preparation

All measurements were carried out under UHV conditions in a residual pressure of about 1×10^{-10} mbar. Thus the surface cleanliness condition achieved at the start of an experiment was not influenced by adsorption from the gas phase constituents during an $I(T)$ measurement.

Pb crystals were cut from a large single crystal ingot by spark erosion. They were oriented to ±15′ from (110) or (111) by Laue back reflection [28]. To obtain good Laue diffraction patterns it was advantageous to cool the crystal by liquid nitrogen. A smooth surface was prepared by combined mechanical and chemical polishing. For chemical polishing, a solution of acetic acid (80%) and hydrogen peroxide (20%) was used. After polishing, the crystal was mounted on the Cu plate and inserted into the UHV system. The degree of surface order and cleanliness of the Pb crystals was judged from LEED and AES, respectively. Sputtering with Xe ions at 1 keV was helpful for improving the quality of LEED patterns and hence surface order. Several cycles of Xe sputtering and flashing up to 580 K produced good LEED patterns. Impurities observed during the initial cleaning were carbon and oxygen. The only persistently recurring impurity, however, was oxygen. When the crystal was cleaned by Xe (or Ar) sputtering at 300 K and heated for prolonged periods at ~ 500 K or briefly up to 570 K and cooled, a small amount of surface oxygen could be detected by AES. Such a sequence is shown in fig. 2. Prior to annealing the crystal was cleaned by sputtering. Traces (a) through (c) are Auger spectra of Pb(110) at temperatures of 470, 520 and 570 K, respectively, during an $I(T)$ measurement cycle up to 590 K. Trace (d) is a spectrum taken after the crystal had cooled down again to 290 K; here 0.33 monolayer of segregated oxygen can be seen. The coverage was estimated by comparison with oxygen on platinum [29]. Oxygen always appeared after the sample had been heated to the vicinity of 570–590 K and then cooled.

This surface oxygen in fig. 2d is due to segregation from the bulk as shown in fig. 3. Here the temperature dependence of the oxygen coverage is plotted during heating (after oxygen was already on the surface) and cooling. The reversibility of this phenomenon is consistent with segregation of oxygen to the Pb(110) surface. Although there is quite a bit of scatter in the data, a segregation energy of -1.3 ± 0.6 eV/atom can be estimated. Similar behavior was also observed for Pb(111).

In the context of the $I(T)$ measurements it is important to note that no oxygen segregation was observed during the first heating period up to 580 K

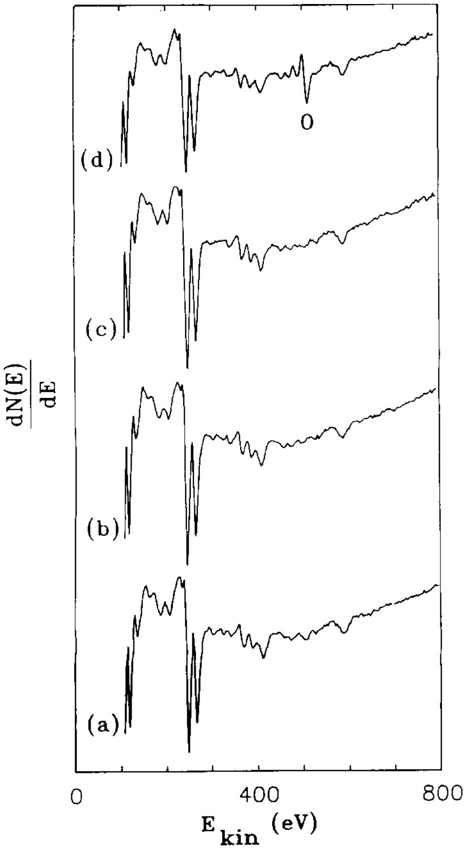

Fig. 2. Auger spectra of Pb(110) taken at several temperatures. (a) 470 K, (b) 520 K, (c) 570 K, (d) after cooling to room temperature.

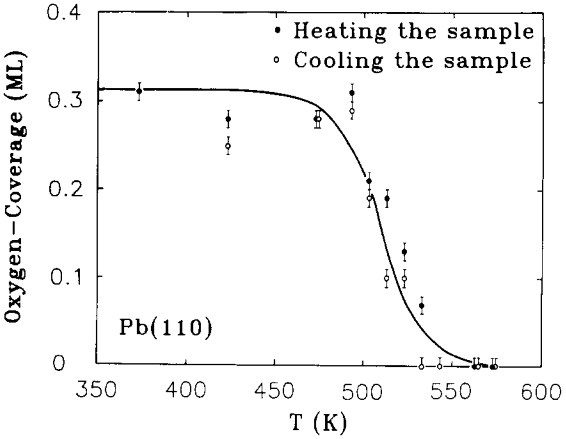

Fig. 3. Relative oxygen coverage versus temperature. Oxygen KVV Auger intensity divided by lead NOO Auger intensity, calibrated by comparison with O/Pt(111) (ref. [28]).

starting with a clean surface. The oxygen appeared only after the first heating and cooling cycle. Therefore we do not expect this segregated oxygen to interfere with the observed surface disordering process.

3. Results

3.1. Visual LEED observations

Photographs of the LEED pattern for the clean Pb(110) surface are shown in figs. 4a–4c for three different temperatures at a primary electron energy of 29 eV. All photographs were taken under the same exposure conditions so that the relative spot and background intensities at different temperatures can be compared. The pattern taken with the crystal at 200 K exhibits sharp and intense spots indicative of excellent surface order. This also holds for the LEED pattern of the Pb(111) surface shown in fig. 4d at the same temperature

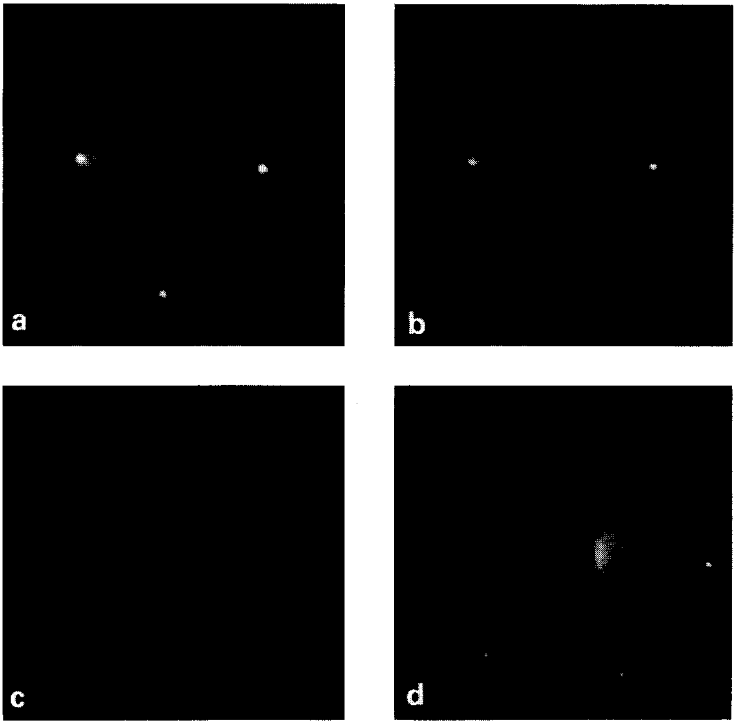

Fig. 4. LEED patterns of Pb(110) and Pb(111) at several temperatures. (a) Pb(110) at 200 K, (b) Pb(110) at 420 K, (c) Pb(110) at 570 K, (d) Pb(111) at 200 K. Primary energy for all patterns is 29 eV.

and energy. Increasing temperature reduces the intensities of the diffraction spots relative to background. This general decrease in spot intensity with rising temperature is due to inelastic electron phonon scattering, i.e. the Debye–Waller effect. It occurs for both Pb(110) and Pb(111) without any obvious difference. On close examination of the LEED pattern for Pb(110) at ~ 570 K, however, it becomes apparent that the diffraction spots have vanished. On the other hand, the LEED pattern for Pb(111) at the same temperature still showed well-defined diffraction spots. The different behavior in spot intensities for these two surfaces under various conditions will become evident in actual $I(T)$ plots in the following section.

3.2. LEED intensity data – Pb(111)

For Pb(111) detailed $I(T)$ curves were measured for (00) and (10) beams at several primary energies. Fig. 5 shows a set of data for the (10) beam. All $I(T)$ curves were fully reversible with temperature. In all cases the intensity decays with increasing temperature; most of the $I(T)$ curve can be fitted to a Debye–Waller exponential expression except at the very lowest energy of 12 eV. Here the decrease of the intensity is nearly linear (see discussion). As important as the beam intensity itself is the relative magnitude of the background and its changes with temperature. These are illustrated for the (00) and (10) beams at $E_p = 19$ eV in figs. 6a and 6b, respectively. The background

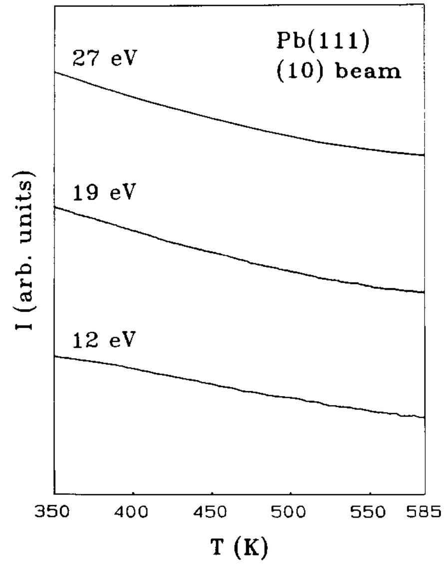

Fig. 5. Intensity versus temperature curves of the (10) beam of Pb(111). The primary energy is shown next to each curve.

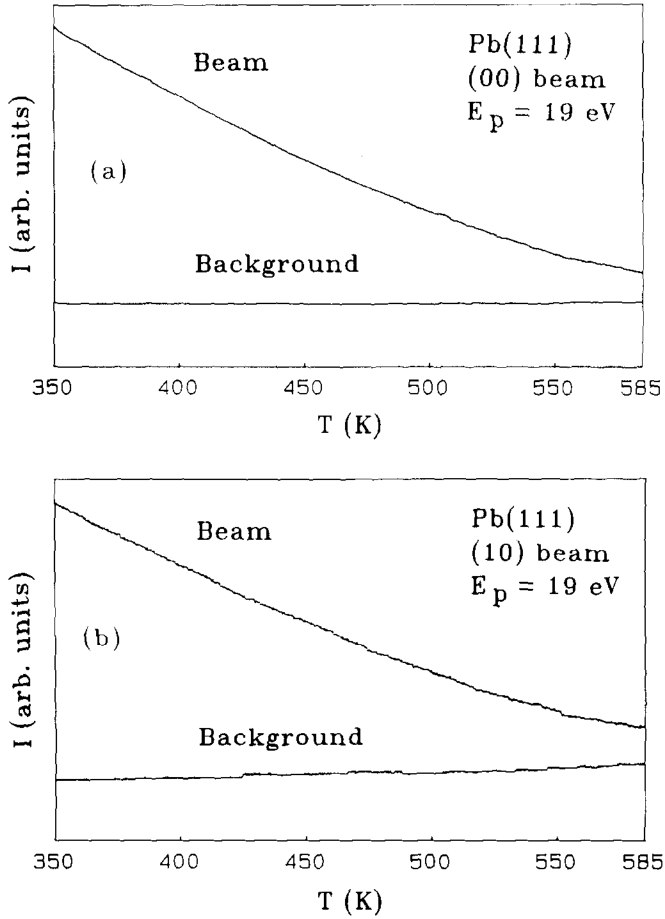

Fig. 6. Intensity versus temperature curves, for Pb(111) and primary energy of 19 eV. (a) Pb(111), (00) beam and background intensity; (b) Pb(111), (10) beam and background intensity.

intensity increases slightly with rising temperature as expected on the grounds of additional elastic and inelastic (phonon) diffuse scattering [30]. On the other hand, the beam intensities at 585 K, the highest temperature in fig. 6, stay well above the background. This means that long-range order on Pb(111) is preserved at least up to 585 K.

Those $I(T)$ traces that were not linear were fitted to an exponential in order to extract an effective Debye temperature [31]. Although the microscopic meaning of such a number is questionable in view of multiple-scattering processes, it is still instructive to compare it with the effective bulk Debye temperature of Pb. This is temperature dependent but an average experimental value for Pb is 88 K [32]. Values of the mean square thermal displacement in

Pb as a function of temperature measured with neutron diffraction [33] also yield Debye temperatures. From these data a mean value of about 80 K for the temperature region 400–500 K is obtained. The apparent surface Debye temperature for Pb(111) is 50 ± 10 K, i.e. it is considerably lower than the bulk value, which is typical for surface Debye temperatures [30].

3.3. LEED intensity data – Pb(110)

Measured $I(T)$ curves for Pb(110) are shown for (00), (01) and (10) beams at several primary beam energies in figs. 7–9, respectively. As with Pb(111), these were recorded during heating as well as cooling and found to be fully reversible. The maximum energy for which $I(T)$ was recorded is 42 eV. Even for this relatively low energy the Debye–Waller factor is already quite large such that the intensity decrease is solely governed by it. This can be seen by comparison of the measured intensities at different temperatures for a particular beam. For example, the ratio of the intensity at 500 and 350 K for the (01) beam at 6.5 and 42 eV yields ~ 0.7 and ~ 0.08, respectively, The (01) beam therefore has about nine times as much residual intensity at 500 K and 6.5 eV compared with 500 K and 42 eV. This comparison is independent of the intensities at low temperatures for these particular energies. In fact there is no

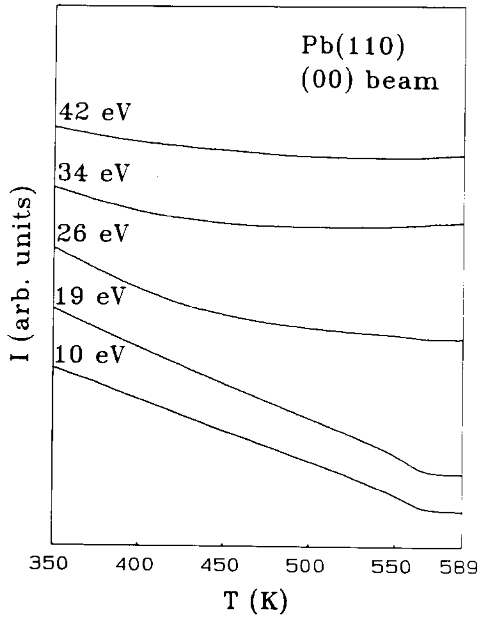

Fig. 7. Intensity of the (00) beam of Pb(110) versus temperature. The primary energy is shown next to each curve.

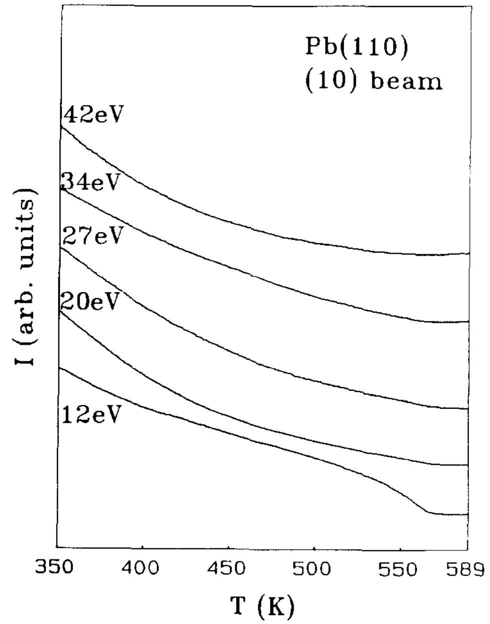

Fig. 8. Intensity of the (10) beam of Pb(110) versus temperature. The primary energy is shown next to each curve.

advantage in looking for a high intensity at low temperature, when the primary electron energy is high because the Debye–Waller factor reduces the intensity quickly with rising temperature.

At lower primary energies the Debye–Waller factor is smaller and effects on the intensity due to disorder are expected to show up more readily. This is in fact the case in figs. 7–9 for energies below ~ 26 eV. The $I(T)$ curves for all three beams exhibit a change in curvature around 520 K resulting in a faster approach to background intensity than obtained from a low temperature extrapolation. The observation that this additional downturn in $I(T)$ at 520–580 K occurs for all three beams and at several kinetic energies indicates that it is unlikely to be due to dynamic effects, for example. We interpret this behavior as direct evidence for a surface-related order–disorder transition.

Higher order beams, such as (11) and (02), were also measured at kinetic energies of 27 and 34 eV with nearly normal incidence (incident angle of the primary beam $\leq 4°$) but the Debye–Waller factor for these beams is higher than for the zeroth- or first-order beams, and no clear effect in $I(T)$ of the kind seen in figs. 7–9 could be detected.

Fig. 10 shows a comparison of measured $I(T)$ for (00), (10), and (01) beams and respective background intensities at 10–12 eV primary energy. The decrease in intensity for (00) at 10 and 19 eV (see also fig. 7) is almost linear,

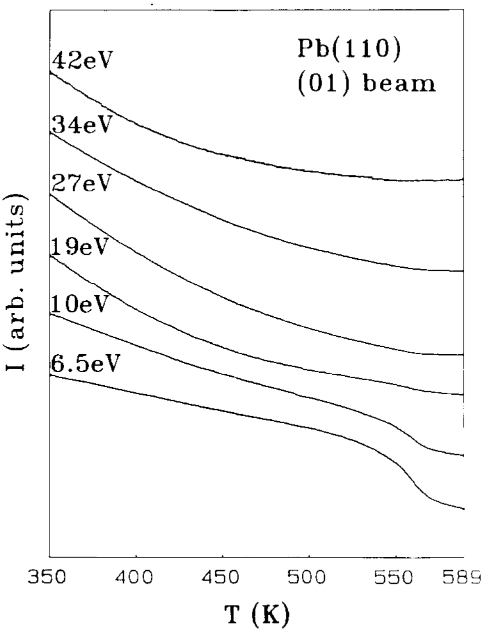

Fig. 9. Intensity of the (01) beam of Pb(110) versus temperature. The primary energy is shown next to each curve.

analogous to Pb(111) for low energies (see fig. 6). A possible explanation for this behavior is given in the discussion. The background intensities in fig. 10 are nearly constant or slightly rising (for the (10) beam) in the measured temperature range. The beam intensities approach the background intensity near 580 K very closely in the case of the (00) and (10) beams, and somewhat less closely for the (01) beam. This behavior is distinctly different from that in fig. 6 for Pb(111), and underlines the presence of a surface phase transition for Pb(110). The detailed approach of the curve to background was found to be characteristically different for (10) and (01) beams, as shown in figs. 10b and 10c. Whereas $I(T)$ for the (10) beam was practically indistinguishable from the background at $T > 580$ K, $I(T)$ for (01) stayed clearly above the background even at 590 K. This difference is indicative of an anisotropic disordering at the Pb(110) surface [34].

The decrease of $I(T)$ at low temperature was generally exponential, i.e. Debye–Waller-like, with the exceptions mentioned above. Hence $I(T)$ curves were fitted to exponentials, and the slopes were evaluated to yield effective Debye temperatures, Θ_D, for the Pb(110) surface, with an average value of about 48 ± 8 K. A comparison of the effective surface Debye temperature for Pb(110) and Pb(111) yields no systematic difference. This is not unexpected because of the influence of multiple scattering that tends to wash out dif-

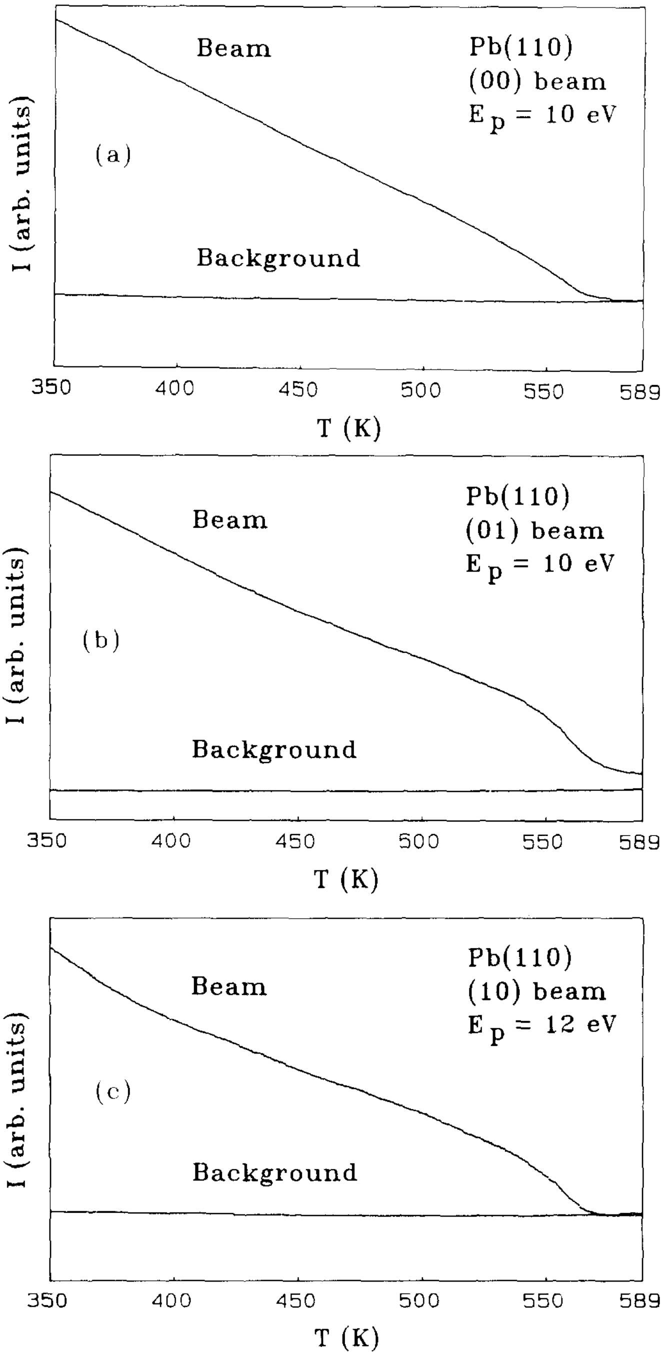

Fig. 10. Beam intensity and background intensity versus temperature for Pb(110). (a) (00) beam, 10 eV primary energy; (b) (01) beam, 12 eV primary energy; (c) (10) beam, 10 eV primary energy.

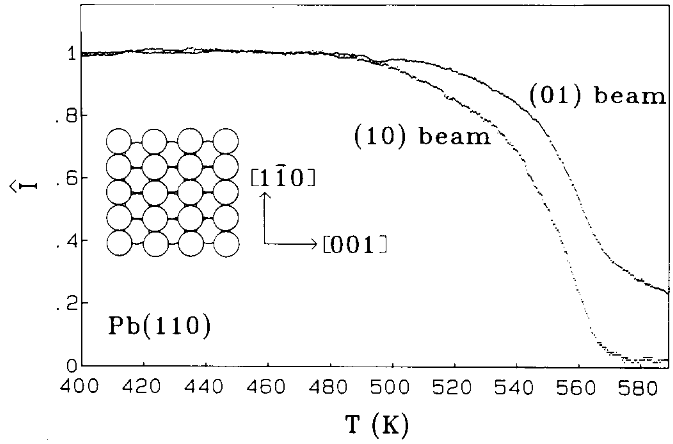

Fig. 11. (10) and (01) beam intensity, corrected for background and the Debye–Waller factor, $I(T)$, versus temperature. For (01) the primary energy is 10 eV; for (10), 12 eV.

ferences between various surface directions; this has been experimentally verified for W(110) [35]. With these fitted exponentials the deviation of $I(T)$ from a normal Debye–Waller decay becomes even more visible [34]. The magnitude of this deviation increases with decreasing kinetic energy, as expected.

The measured $I(T)$ curves were corrected for background and the Debye–Waller effect by calculating

$$\hat{I}(T) = \frac{I(T) - I_{BG}(T)}{I_{DW}(T)}, \tag{1}$$

where $\hat{I}(T)$ is the corrected intensity, $I_{BG}(T)$ the temperature dependent background intensity and $I_{DW}(T)$ the Debye–Waller function fitted to the data. The corrected intensity, which is proportional to the square of the order parameter (see following section), is plotted in fig. 11 for (10) and (01) beams at low kinetic energy. The reduced intensity function is unity up to about 480 K and starts to decrease towards higher temperatures. The rate of decrease is considerably larger for the (10) than for the (01) beam. The decrease for the (10) beam is to near zero intensity while that for the (01) beam is rather incomplete at 590 K indicative of residual order in the [001] azimuth of the Pb(110) surface. Thus the data in fig. 11 illustrate more clearly the directional anisotropy in disordering of the surface [34]. The effect of anisotropy was also detectable at higher kinetic energies but it was less pronounced.

4. Evaluation

In this section we carry out a simple evaluation of our experimental results in terms of the theory presented separately [36]. We first summarize the latter and then derive specific formulas for the case of LEED.

4.1. Thickness of disordered layer and surface order parameter

For the phase transition from a crystalline solid to a liquid which occurs at the melting temperature T_m, premelting may exist and be characterized by a disordered surface layer of thickness l between the crystalline solid and its vapor phase [36–42]. The thickness l of the disordered layer pictured in fig. 12a is a unique function of temperature for $T < T_m$. Such a layer will exist if the interfacial and bulk energies connected with it are lower than the corresponding energies of the crystalline solid at T. The phase transformation from a crystalline solid to a liquid involving a disordered or quasi-liquid layer of finite thickness l is a continuous order–disorder transition [37]. It is characterized by an order parameter function, which shows a continuous loss of order from a finite value in the solid to a low value at the "liquid/vapor" interface, i.e. at the surface.

For surfaces of 2-fold symmetry, e.g. for fcc (110), one may expect that the process of surface disordering or "melting" is not isotropic but dependent on the azimuthal direction. Recent theory of the order parameter for semi-infinite systems has shown [36] that the order parameter function can be expressed as a series involving the parallel components of all reciprocal lattice vectors, $\boldsymbol{Q}_j^{\parallel}$:

$$M(\boldsymbol{x}, z) = M^{(0)}(z) + \sum_j \tilde{M}\left(\boldsymbol{Q}_j^{\parallel}, z\right) \exp\left(\mathrm{i}\boldsymbol{Q}_j^{\parallel} \cdot \boldsymbol{x}\right), \tag{2}$$

where $\boldsymbol{x} = (x_1, x_2)$ and z are coordinates parallel and perpendicular to the surface, and $M^{(0)}(z)$ is a particle number density. The coefficients $\tilde{M}(\boldsymbol{Q}_j^{\parallel}, z)$ are order parameter components describing the decrease in order as a function of z but for a particular direction $\boldsymbol{Q}_j^{\parallel}$ parallel to the surface. The fact that only parallel components of $\boldsymbol{Q}_j$ appear in this series is a consequence of the translational invariance of layer particle densities [36]. The z-dependence of each order parameter component is governed by a characteristic length parameter a_j ("correlation length") that is approximately equal to the inverse of $|\boldsymbol{Q}_j^{\parallel}|$ [36].

Eq. (2) can be viewed as a Fourier series where the Fourier components are the transform of the z-dependent layer densities parallel to the surface. In a typical situation the first few terms are expected to be dominant. If $\boldsymbol{Q}_j^{\parallel}$ is given by the general form

$$\boldsymbol{Q}_j^{\parallel} = n_1 \boldsymbol{q}_1 + n_2 \boldsymbol{q}_2, \tag{3}$$

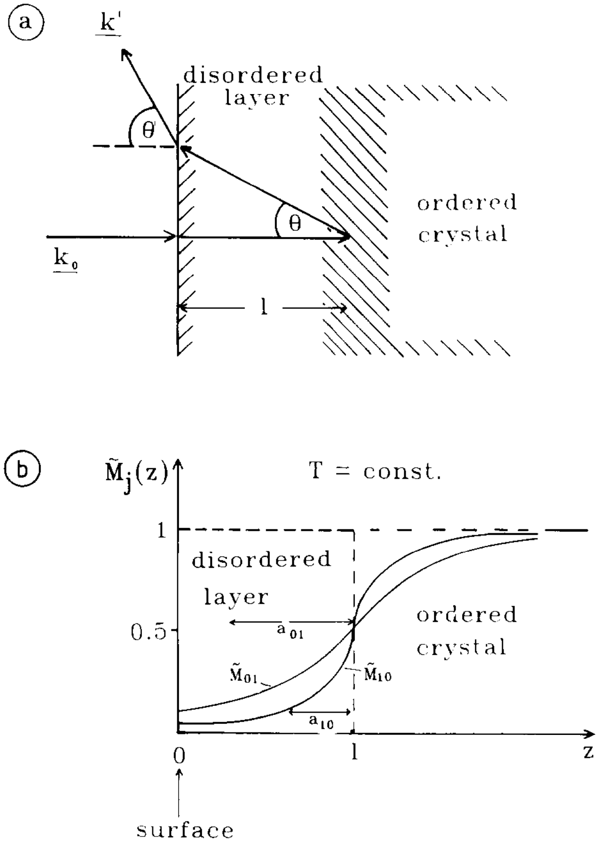

Fig. 12. Model for the diffraction from an ordered crystal with disordered overlayer. (a) Schematic diagram for scattering in the disordered overlayer. Electrons incident with momentum $\boldsymbol{k}_0$ are scattered by an angle θ in the solid and emerge with momentum $\boldsymbol{k}'$ at angle θ'. l is the thickness of the disordered layer. (b) Schematic diagram of the order parameter components $\tilde{M}_{10}(z)$ and $\tilde{M}_{01}(z)$ versus depth z into the solid at constant temperature. a_{10} and a_{01} are lengths characteristic of the decay of order as a function of distance from the interface, i.e. correlation lengths associated with $\tilde{M}_{10}$ and $\tilde{M}_{01}$, respectively.

where $\boldsymbol{q}_1$, $\boldsymbol{q}_2$ are base reciprocal vectors defined by $\boldsymbol{r}_k \cdot \boldsymbol{q}_l = 2\pi\delta_{kl}$ $(k, l = 1, 2)$, with $\boldsymbol{r}_1$ and $\boldsymbol{r}_2$ as base vectors in real space in $\langle 110 \rangle$ and $\langle 001 \rangle$ directions parallel to the surface. n_1 and n_2 are integers. The leading terms in the Fourier series are those with (n_1, n_2) either (1, 0) or (0, 1). These two terms corresponds to the experimentally measured LEED beams (10) and (01). Hence we define the order parameter component $\tilde{M}_{01}(z) = \tilde{M}(\boldsymbol{Q}_{01}^{\|}, z)$ and $\tilde{M}_{10}(z) = \tilde{M}(\boldsymbol{Q}_{10}^{\|}, z)$ where $|\boldsymbol{Q}_{01}^{\|}| = 2\pi/d$ and $|\boldsymbol{Q}_{10}^{\|}| = 2\pi\sqrt{2}/d$ (d: lattice parameter). We expect these to be the most significant for the continuous order/disorder transition.

The order parameter components $\tilde{M}_{01}(z)$ and $\tilde{M}_{10}(z)$ can be approximated by the following expression:

$$\tilde{M}_j(z) = \tilde{M}_j^0 \begin{cases} \frac{1}{2} \exp\left[-(l-z)/a_j\right], & z \leq l, \\ 1 - \frac{1}{2} \exp\left[-(z-l)/a_j\right], & z > l, \end{cases} \quad j = (01), (10), \tag{4}$$

where a_{01} and a_{10} are the corresponding correlation lengths in $\langle 001 \rangle$ and $\langle 1\bar{1}0 \rangle$ directions and $\tilde{M}_j^0$ are the prefactors of the individual order parameters. The exponential decay in eq. (4) given here for the order parameter components is valid as long as long-range forces are not important.

Because of the reciprocity relationship between a_j and $\boldsymbol{Q}_j^{\|}$ [36] it follows that the leading terms (fundamentals) of the Fourier series are linked to the most slowly varying $\tilde{M}_j$ components because the resulting a_j are the largest. This is important from an experimental point of view because slow variations in $\tilde{M}_j(z)$ are connected with extended regions of residual order, and hence give rise to large measured signals, e.g. in LEED. In other words, the most slowly varying $\tilde{M}_j(z)$ component, for a given $\boldsymbol{Q}_j^{\|}$ direction, will be dominant in the diffraction signal from that particular direction.

Any diagnostic tool that allows one to study the degree of order along a certain crystallographic direction, e.g. [001], will provide information about the order parameter profile along this direction, and – if disordering occurs at high temperature – also about the thickness l of the disordered layer. Tools probing long range order should in principle be suitable for this task. However, this simple picture is only correct in the ideal case of kinematic scattering and parallel momentum transfer. Both of these conditions are not fulfilled in LEED. Therefore we cannot expect LEED beams to describe exclusively a particular direction but some degree of mixing from other directions (beams) will be present. Despite this, a certain amount of directional anisotropy information might still be preserved, for example, in the behavior of (10) and (01) beams.

For the experimental evaluation it is important to know the temperature dependence of the thickness of the disordered or quasi-melted layer. This is obtained theoretically by considering the direct interaction between the two interfaces bounding the layer [36,43]. These interfaces are assumed to be planar, i.e. fluctuations are not taken into account. The direct interaction energy involves short range as well as long range force terms [41,42] which generally give rise to either a logarithmic or a power law dependence of the thickness on temperature. Both types of growth law have been established experimentally for Pb(110) crystals near the bulk melting point [10,14]. The experimental data indicate that the logarithmic growth law

$$l(T) = c a_0 \ln\left(\frac{\Delta T}{T_m - T}\right), \quad \Delta T = T_m - T_0, \tag{5}$$

where T_0 is the onset temperature for disordering, prevails at temperatures further removed from T_m, i.e. at $T_m - T > 0.3$ K [14]. Some difficulty arises with respect to the constant c in eq. (7) which was taken to be either unity or 0.5 [10,14,34]. Theoretically, there is as yet no unambiguous rule for the choice of c although a detailed derivation of formulas and related discussion were given elsewhere [36]. Recent experiments of Pb(110) surface disordering utilizing X-ray photoelectron diffraction (XPD) have indicated a change in growth law with temperature [44]. At temperatures of 520–575 K the data are described by the logarithmic growth law with $c = 1$ and above 575 K with $c = 0.5$ [44]. Based on these findings we select $c = 1$ for the evaluation of the present LEED data because the usable temperature range is here about 550–570 K (fig. 11). The use of $c = 1$ is also consistent with previous work [34] which has yielded a reasonable interpretation of the data. Furthermore the use of $c = 1$ does not contradict the evaluation of a most recent RBS study of Pb(110) surface melting [14] because there is little overlap in the temperature ranges. The growth law with $c = 0.5$ was found to prevail for the range 560–600 K in the RBS study [14] while here $c = 1$ is applied for the range below 570 K. Also, there is consistency between this recent RBS work and the evaluation of XPD measurements for $T > 575$ K mentioned above [44].

Theoretically, the logarithmic growth law with $c = 0.5$ has been derived for temperatures close to T_m, i.e. for large $l(T)$ [36]. It is not clear whether the same formula derived for this condition would also hold far away from the triple point, i.e. for small $l(T)$. Hence the demand of $c = 1$ for small $l(T)$ is by no means in contradiction with theory. In fact, a cross-over from $c = 1$ to $c = 0.5$ at lower temperatures is possible if, for example, the prefactors of the exponential terms that govern the direct short range interaction between the "crystal liquid" and the "liquid/vapor" interfaces [36] would be weakly temperature dependent. A more complete theory of this interaction might be able to shed light on this question.

4.2. LEED intensity of diffracted beams

As shown schematically in fig. 12b, the degree of order in the disordered surface film of thickness l increases from the surface towards the ordered crystal. If an electron beam enters at normal incidence, fig. 12a, diffraction in the disordered film as well as the ordered crystal will occur with intensity depending on $\tilde{M}(z)$. We assume a very simple model in which each layer will independently contribute to the diffracted intensity according to its degree of order. This is a rather crude approximation because it neglects the contributions from the interference of the beams between the layers. We take into account that the diffracted intensity from within the solid will be damped by outer layers.

Based on fig. 12a, let us consider a diffracted beam emerging at the angle θ' outside the solid and θ inside. θ is determined by the primary energy and calculated using Bragg's Law. θ' is obtained by considering refraction at the surface. Let $I'(z_n)$ be the intensity which originates from a layer at depth z_n below the surface. Then the escape depth will be $z_n/\cos\theta$. Assuming that the intensity decrease is governed by an electron mean free path λ, which includes inelastic and diffuse elastic scattering of the electrons, we have

$$\hat{I}(z_n) = I'(z_n)\exp(-z_n/\lambda\cos\theta). \tag{6}$$

However, the incident beam also has to penetrate up to depth z_n so that it will be damped by a factor $\exp(-z_n/\lambda)$. This factor will multiply the diffracted intensity from depth z_n. The total diffracted intensity in direction θ is obtained by summation over all layers:

$$I = \sum_n I(z_n) = \sum_n I'(z_n)\exp\left[-\frac{z_n}{\lambda}\left(1+\frac{1}{\cos\theta}\right)\right]. \tag{7}$$

This expression describes the intensity of a diffracted beam after corrections for background and the Debye-Waller factor [34].

We now assume that the intensity $I'(z_n)$ is equal to the square of the order parameter at z_n, $\tilde{M}_j^2(z_n)$, which according to section 4.1 is expected to be anisotropic and to depend on the azimuth of observation. Since we are in particular interested in deriving an expression for the temperature dependence of diffracted intensities for the (10) and (01) beams, i.e. corresponding to the orthogonal directions [1$\bar{1}$0] and [001] in real space, we take into account the order parameter components for these two directions, eqs. (4) as explained above and elsewhere [34]:

$$I_j(T) = A\sum_{n=0}^{\infty}\tilde{M}_j^2(z_n)\exp(-z_n f/\lambda), \quad j=(01),(10), \tag{8}$$

with $f = 1 + (\cos\theta)^{-1}$ and $z_n = nd/2\sqrt{2}$, d is the lattice parameter of Pb (4.95 Å). A is a normalization constant with $A = 1 - \exp(-df/2\sqrt{2}\cdot\lambda)$. This arises from the condition $I_j = 1$ for the completely ordered crystal. Inserting eq. (4), we obtain for the normalized intensity

$$\begin{aligned} I_j(T) = {}& \tfrac{1}{4}A\sum_{n=0}^{n'}\exp\left(-\frac{2(l(T)-z_n)}{a_j}-\frac{z_n f}{\lambda}\right) \\ &+ A\sum_{n=n'+1}^{\infty}\left[\exp\left(-\frac{z_n f}{\lambda}\right)-\exp\left(-\frac{z_n-l(T)}{a_j}-\frac{z_n f}{\lambda}\right)\right. \\ &\left.+\tfrac{1}{4}\exp\left(-\frac{2(z_n-l(T))}{a_j}-\frac{z_n f}{\lambda}\right)\right], \quad l(T)\geq 0, \quad T\geq T_0, \end{aligned} \tag{9}$$

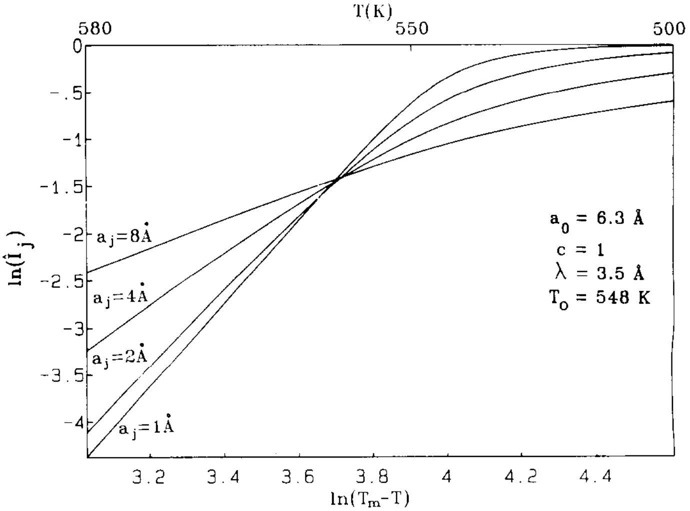

Fig. 13. Logarithm of the calculated intensity, $\ln(\hat{I}_j)$ versus $\ln(T_m - T)$ for one example of parameters $a_0 = 6.3$ Å, $c = 1$, $\lambda = 3.5$ Å and $T_0 = 548$ K. T_m and T are the melting temperature and the sample temperature, respectively. a_j is shown next to each curve.

where $n' \leq 2\sqrt{2}\, l(T)/d$. The finite summation until n' in the first term arises from the condition $z_n \leq l(T)$. The temperature dependent thickness $l(T)$ of the disordered layer is given by eq. (5). In our model the order parameter $\tilde{M}_j(z=0)$ has the value 1/2 for $l(T) = 0$ or $T = T_0$. So the state of a fully ordered crystal with $\tilde{M}_j(z=0) = 1$ is reached asymptotically for low temperatures, which corresponds to the extrapolation $l(T) < 0$ for $T < T_0$ and $n' = 0$ in eq. (9). Therefore in this case the only contribution to the intensity arises from the second sum in eq. (9). By evaluating the expressions in eq. (9), which are sums of geometric series, and inserting eq. (5), we obtain in the case $T \geq T_0$

$$I_j(T) = k_1 \left(\frac{T_m - T}{T_m - T_0} \right)^{2ca_0/a_j} + k_2 \left(\frac{T_m - T}{T_m - T_0} \right)^{fca_0/\lambda}, \tag{10}$$

where k_1, k_2 are constants depending on a_0, a_j, d, f, c and λ. We have previously obtained the same functional dependence within a continuum model, where the sums are replaced by integrals [34]. The layer model changes only the values of the constants k_1 and k_2.

Under the limiting conditions $2a_0c/a_j \gg 1$, $\lambda/a_j > 1$ for the relative values of a_0, a_j, c and λ, it can be shown that the *second* term dominates in eq. (10). For our model, we have calculated eq. (10) numerically using a range of suitable values. Fig. 13 shows a plot of the logarithm of intensity versus the logarithm of $(T_m - T)$ for one set of values ($a_0 = 6.3$ Å, $c = 1$, $\lambda = 3.5$ Å, $T_0 = 548$ K, $a_j = 1, 2, 4, 8$ Å). For values $a_j \leq 2$ Å the curves are straight lines

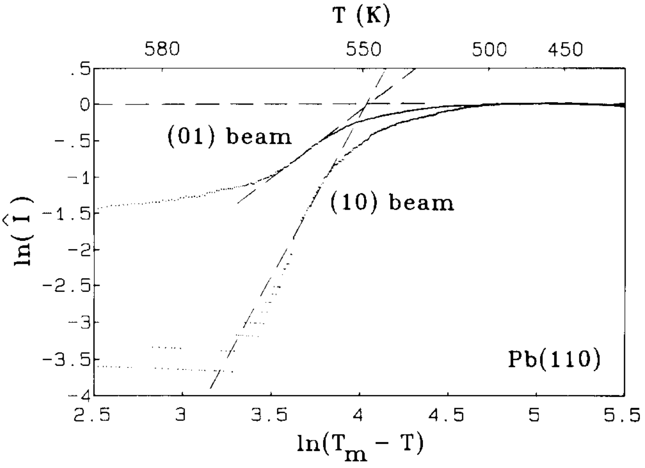

Fig. 14. Logarithm of the intensity, corrected for background and Debye–Waller effects, ln $\hat{I}(T)$, versus $\ln(T_\mathrm{m} - T)$, for (10) and (01) beams at 12 and 10 eV primary energy, respectively.

well above the onset temperature T_0 and have a slope of $a_0 fc/\lambda$. The experimental value of the slope for the (10) beam at 12 eV primary energy is 5 ± 1, as can be seen in fig. 14. The value of f is 2.5 at 12 eV, calculated with an inner potential of 10 eV. A reasonable value for a_0 is 6.3 Å [14], giving a value of λ of 3.5 Å. For these values and certain ratios of a_0/λ we have compared our model function in eq. (10) with the experimental data. In fig. 15 we show a comparison for the values $a_0 = 6.3$ Å, $\lambda = 3.5$ Å, $T_0 = 548$ K and different a_j between 0.5 and 3 Å. The best fit in the temperature region of the onset temperature T_0 is reached for $a_{10} = 1.75$ Å which is comparable to the layer spacing for Pb(110). For higher temperatures the evaluated curves are independent of a_{10} as predicted. These results may be compared with the theoretical prediction of a_{10} [36]:

$$a_{10} = \frac{a_0}{\left[1 + \left(a_0 Q_{10}^{\|}\right)^2\right]^{1/2}} \approx \frac{1}{Q_{10}^{\|}} = 0.56\ \text{Å},$$

where a_0 is the correlation length within a bulk liquid. The theoretical value of a_{10} is lower than the best fit value of the experiment. This may be due to the difference between the continuum model and reality. In reality the width of the interface between the liquid and the crystal phase should be of the order of a layer spacing.

The situation is different for the (01) beam intensity. The double-log plot in fig. 14 for the (01) beam exhibits two separate regions with a crossover at about 570 K. New XPD measurements confirm that the appearance of two separate regions in fig. 14 is genuine and that the crossover is due to a change

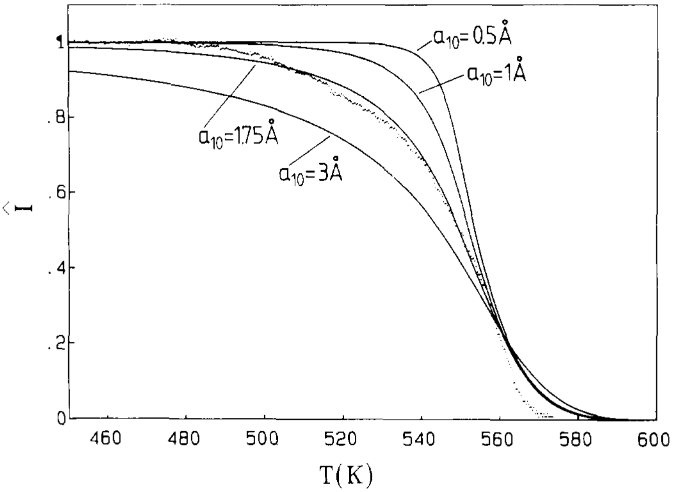

Fig. 15. Comparison of the measured and calculated intensity $\hat{I}_{10}(T)$ versus temperature T. Parameters for the calculation are $a_0 = 6.3$ Å, $c = 1$, $\lambda = 3.5$ Å, $T_0 = 548$ K, a_{10} is shown next to each curve.

in growth kinetics of the disordered layer [44]. Obviously such a crossover should also be visible in the (10) beam at the same temperature but the anisotropy of the disordering process results in a faster decrease of intensity for the (10) beam which prevents the detection of this crossover. A detailed examination of the slope of the (01) beam in the first region, indicated by a straight line in fig. 14, is difficult in terms of eq. (10). The value of 1.7 ± 0.5 for the slope indicates that the limiting condition $2ca_0/a_j \gg 1$ in eq. (10) is not fullfilled so that both terms in this equation contribute to the intensity in this temperature region. As a consequence, the interface in the corresponding [001] direction cannot be as sharp as in the [1$\bar{1}$0] direction [34].

5. Discussion

The comparison of temperature dependent LEED beam intensities of Pb(111) and Pb(110) shows unequivocally an anomalous decrease for $T > 480$ K for Pb(110). All investigated beams exhibit this decrease for various primary energies although the effect is most pronounced at the lowest possible primary energies. This anomalous decrease in beam intensity is taken as evidence for a surface order–disorder transition.

At some energies, for both the (111) and (110) surfaces, the decrease in intensity for temperatures below 480 K did not follow the expected

Debye–Waller exponential curve, but was more like a straight line. There are two possible reasons for this. Firstly the effect may be due to anomalous thermal expansion of the first layer with respect to the second, which is reported to be about 15% [45]. Such a large change alters the diffraction conditions and may in general lead to higher or lower intensity. This suggestion could be tested by measuring the thermal expansion on Pb(111) which should be similar to Pb(110) if this is the origin of the effect.

A second possibility is the presence of anharmonicity. From neutron scattering of bulk Pb [33], it is known that the atomic mean square displacement increases faster with rising temperature than expected on the basis of a harmonic oscillator. This implies that in the bulk an anharmonic potential is necessary to describe the thermal effects in diffraction. At a surface, anharmonic effects are expected to be larger because the lower coordination number enhances the vibrational amplitude. Anharmonicity may also be responsible for the rather gradual decrease of ~ 20% in intensity between 480 and 540 K. It cannot however explain the much larger decrease of ~ 50% between 540 and 570 K, as this is much too large for such a narrow temperature range.

Most interesting is the clearly visible anisotropic behavior of $I(T)$ for (10) and (01) beams at $T > 480$ K. This anisotropy was present for various primary energies and cannot be attributed to a dynamic LEED effect. It appears to be a true characteristic of the disordered surface layer forming at $\Delta T \approx 100$ K below the bulk melting point of Pb. In that sense the anisotropy of disorder distinguishes this surface layer from a three-dimensional liquid. On the basis of the present data it seems realistic to expect the surface order parameter for the [001] and [1$\bar{1}$0] azimuths, to vanish simultaneously for $T = T_m$ but with different critical exponents which reflects the basic anisotropy. This is an agreement with theory [36] which predicts that all order parameter components should vanish at the surface when complete surface melting occurs.

As a consequence of the anisotropy in disordering the transition width for the order parameter is quite different for [001] and [1$\bar{1}$0] directions, as expected on theoretical grounds (compare section 4.2). With regard to specific values there is good evidence for a sharp transition ($a_{10} = 1.75$ Å) in the [1$\bar{1}$0] direction, i.e. for disordering along the rows of close-packed atoms [34]. The sharpness of this transition can qualitatively be derived from the $I(T)$ curve for the (10) beam in fig. 11. Here the intensity decreases rather steeply into the background. This means that no diffracted (10) intensity from either the ordered crystal or the disordered layer reaches the detector at $T \geq 570$ K. This is only possible if the order within the layer for this azimuth is lost, and if the (10) intensity from the underlying ordered crystal is completely attenuated by the disordered overlayer. This corresponds to an overlayer thickness of about $2\lambda \approx 7$ Å. If the order parameter decreases from unity to zero within about $l = 7$ Å the transition width can only be a fraction of that, e.g. 20–30%. In other words, the transition must have a sharp boundary, in agreement with the evaluation.

How can the anisotropy of disordering be envisioned? The atoms in the $[1\bar{1}0]$ rows of a Pb(110) surface are sitting in troughs perpendicular to the [001] direction. Their coordination number is 7 (nearest neighbors), only one higher than a kink atom. Hence the energy of formation of a terrace vacancy in terms of a nearest neighbor model is equal to the energy of just one bond (about 0.34 eV for Pb). Based on this energy, the concentration of vacancies near T_m would not be much higher than about 0.002. This concentration is too low for explaining a one-dimensional disordering of atoms within the $[1\bar{1}0]$ rows. On the other hand, surface roughening and hence a much larger increase in the concentration of adatoms and terrace vacancies than based on the extrapolation from low temperatures is expected to precede a surface melting process. Indeed, evidence for the surface roughening of a Pb(110) face comes from the observation of equilibrium particle shapes at high temperatures. Heyraud and Métois [46] evaluated the temperature dependent anisotropy of the surface free energy from these observations and found that the cusp at the {110} orientation along the ⟨100⟩ zone vanishes between 548 and 573 K. The disappearance of a cusp is theoretically equivalent to a surface roughening transition [47]. Under the conditions of a surface roughening transition a large increase in the concentration of terrace vacancies and adatoms would occur. The localization of surface atoms not yet displaced by roughening is governed by the diffusional barriers in the ⟨110⟩ and ⟨001⟩ directions. Diffusional motion of atoms in the ⟨110⟩ directions is a very likely event because the activation energy for surface diffusion in this direction is low, as opposed to that in the ⟨001⟩ direction [48]. A sufficient number of surface vacancies will hence enable one-dimensional disordering in the ⟨110⟩ direction before any substantial disorder along ⟨001⟩ occurs.

The process just described for the first layer will also apply for subsequent layers. Since the corrugation of the potential in the ⟨001⟩ direction is larger than in the ⟨110⟩ direction, the perfectly ordered substrate will exert a longer range influence for order in the ⟨001⟩ direction.

The disordering of the surface is a completely reversible process [9,10,14] because perfect order is regained on cooling. This means that a clear structural relationship between ordered and disordered surface layers exists at all $T < T_m$ such that single crystallinity is always achieved on cooling. Of course, because of reversibility the transition boundary during cooling moves towards the free surface leaving perfectly ordered layers behind. The thickness $l(T)$ of the disordered layer is a unique function of temperature, different from three-dimensional melting which occurs isothermally. Thus there are definite structural and thermodynamic differences between the disordered surface layer and the three-dimensional melt. In this sense a term such as quasi-liquid formation is more exact than "surface melting".

Macroscopically, the disordered surface may be a precursor for bulk melting. The rarity of superheating above the melting temperature has often been cited as an indicator that surface disordering occurs. Conversely, since the (111) surface does not disorder, it should be possible to superheat a crystal with only (111) surfaces. This has indeed been elegantly demonstrated by Spiller for small lead crystallites [49].

Because the disordered surface layer is structurally not identical with a three-dimensional liquid, its properties are not expected to be identical. This pertains in particular to surface self-diffusion, as was pointed out years ago [18,19]. In this context it is interesting that surface self-diffusion of Pb(110) has recently been studied by He atom scattering [12]. Here the energetic width of the scattered beam was used to extract the surface self-diffusion coefficient as a function of temperature up to $T/T_m \approx 0.9$ for both [001] and [$1\bar{1}0$] directions. It was noted that there was a small directional anisotropy of diffusion in this temperature range, and that the surface self diffusion coefficient exceeded that of a bulk liquid at 50 K below T_m [12]. The latter feature was taken as evidence for a liquid-like surface at this temperature and above. On the other hand, both features have been observed for other fcc metals before in mass transport experiments [48]; it can be shown that the difference between mass transport and intrinsic surface self-diffusion is not of primary concern [48] for this argument. If a mass transfer surface self-diffusion coefficient larger than 10^{-5} cm^2/s is measured at $T < T_m$ [12] the intrinsic diffusivity should be higher by a factor of the reciprocal adatom concentration. In fact, for Cu(110) mass transfer surface self-diffusion coefficients up to 7×10^{-4} cm^2/s have been measured [50], and since the adatom concentration is unlikely to exceed 10^{-1}, the intrinsic surface diffusion coefficient must be at least 7×10^{-3} cm^2/s, i.e. 300 times larger than bulk liquid diffusion coefficients at T_m. The fact that such large diffusion coefficients exist is likely to be a consequent of the two-dimensional nature of the surface in the first place, and only due to the degree of surface order in the second place [50].

The comparison of our present results with those of previous studies of Pb(110), Pb(111) and other orientations [9–14,16] is interesting. The oldest investigation by Goodman and Somorjai [16] was also carried out using LEED. No effects of surface disordering below T_m were reported for either low-index Pb surface. Effective Debye temperatures of Pb(111) and Pb(110) quoted in their paper [16] are similar to ours but no $I(T)$ curves were published. We have no obvious explanation for the basic discrepancy in the results.

To the extent that we can compare our data with the RBS studies [9–11,14], there is agreement. In fact, we have used the correlation length l_0 from their work [14] to evaluate our $\hat{I}(T)$ plots. The RBS data do not allow any conclusion with respect to the anisotropy of disordering.

A most recent study by X-ray scattering [13] claims the presence of "liquid layers" on Pb(110) and Pb(111) at substantially lower temperatures than in any other investigation of Pb. Liquid layer scattering is supposed to occur at 300 and 220 K for Pb(110) and Pb(111), respectively [13]. In our opinion these results cannot be reconciled with either RBS [9–12,14] or the present LEED results [34].

In summary, our experiments have revealed substantial surface disordering and melting on Pb(110) but not on Pb(111). The results for Pb(110) show an anisotropy of the disordering process [34], which has been theoretically explained in the context of phenomenological Landau models [36]. Much remains to be done both experimentally and theoretically. From a theoretical point of view, a promising approach is density functional theory as has been applied to the problem [51].

Acknowledgement

We gratefully acknowledge the excellent preparation of Pb single crystals by Udo Linke and a pre-print of ref. [14] sent to us by Dr. Bart Pluis.

References

[1] L.S. Palatnik and V.S. Zorin, Soviet J. Phys. Chem. 33 (1959) 191; Zh. Fiz. Khim. 33 (1959) 859.
[2] N.T. Gladkich, R. Niedermayer and K. Spiegel, Phys. Status Solidi 15 (1966) 181.
[3] J. Henrion and G.E. Rhead, Surface Sci. 29 (1972) 20.
[4] G. Devaud and R.H. Willens, Phys. Rev. Letters 57 (1972) 2683.
[5] R.H. Willens, A. Kornblit, L.R. Testardi and S. Nakahara, Phys. Rev. B 25 (1982) 290.
[6] K.D. Stock and E. Menzel, Surface Sci. 61 (1976) 272; J. Crystal Growth 43 (1978) 135.
[7] G. Fritsch and E. Lüscher, Phil. Mag. A 48 (1983) 21.
[8] G. Fritsch, H. Diletti and E. Lüscher, Phil. Mag. A 50 (1984) 545.
[9] J.W.M. Frenken and J.F. van der Veen, Phys. Rev. Letters 54 (1985) 134.
[10] J.W.M. Frenken, P.M.J. Marée and J.F. van der Veen, Phys. Rev. B 34 (1986) 7506.
[11] B. Pluis, A.W. Denier van der Gon, J.W.M. Frenken and J.F. van der Veen, Phys. Rev. Letters 59 (1987) 2678.
[12] J.W.M. Frenken, J.P. Toennies and Ch. Wöll, Phys. Rev. Letters 60 (1988) 1727.
[13] P.H. Fuoss, L.J. Norton and S. Brennan, Phys. Rev. Letters 60 (1988) 2046.
[14] B. Pluis, T.N. Taylor, D. Frenkel and J.F. van der Veen, to be published.
[15] P. von Blanckenhagen, W. Schommers and V. Voegele, J. Vacuum Sci. Technol. A 5 (1987) 649.
[16] R.M. Goodman and G.A. Somorjai, J. Chem. Phys. 52 (1970) 6325.
[17] P. Thiry, G. Jezequel and Y. Petroff, J. Vacuum Sci. Technol. A 5 (1987) 892.
[18] H.P. Bonzel and N.A. Gjostein, Surface Sci. 22 (1970) 216.
[19] G.E. Rhead, Surface Sci. 22 (1970) 223.
[20] G.E. Rhead, Surface Sci. 15 (1969) 353.
[21] D. Nenow, Progr. Crystal Growth Characterization 9 (1984) 185, and references therein.

[22] J.F. van der Veen, in: Chemistry and Physics of Solid Surfaces, Vol. VII, Eds. R. Vanselow and R. Howe (Springer, Berlin, 1988).

[23] Da-Ming Zhu and J.G. Dash, Phys. Rev. Letters 57 (1986) 2959; Phys. Rev. Letters 60 (1988) 432.

[24] N. Greiser, G.A. Held, R. Frahm, R.L. Greene, P.M. Horn and R.M. Sutter, Phys. Rev. Letters 59 (1987) 1706.

[25] J. Bösiger and S. Leutwyler, Phys. Rev. Letters 59 (1987) 1895.

[26] E.G. McRae and R.A. Malic, Phys. Rev. Letters 58 (1987) 1437.

[27] U. Breuer, G. Schmidt, K.C. Prince, K. Heinz, K. Müller and H.P. Bonzel, unpublished work.

[28] U. Linke and B. Poelsema, J. Phys. E (Sci. Instrum.) 18 (1985) 26.

[29] G. Pirug, G. Brodén and H.P. Bonzel, in: Proc. Seventh Intern. Conf. on Solid Surfaces, Vienna, Austria, 1977.

[30] M.G. Lagally, in: Surface Physics of Materials, Vol. 2, Ed. J.M. Blakely (Academic Press, New York, 1975) p. 419.

[31] G.A. Somorjai and H.H. Farrell, Advan. Chem. Phys. 20 (1972) 215.

[32] N.W. Ashroft and N.D. Mermin, Solid State Physics (Holt, Rinehart and Winston, New York, 1976) p. 461.

[33] M. Merisalo, M.S. Lehmann and F.K. Larsen, Acta Cryst. A 40 (1987) 127.

[34] K.C. Prince, U. Breuer and H.P. Bonzel, Phys. Rev. Letters 60 (1988) 1146.

[35] P. Heilmann, K. Heinz and K. Müller, Surface Sci. 89 (1979) 84.

[36] R. Lipowsky, U. Breuer, K.C. Prince and H.P. Bonzel, Phys. Rev. Letters 62 (1989) 913.

[37] R. Lipowsky, Phys. Rev. Letters 49 (1982) 1575.

[38] J.Q. Broughton and G.H. Gilmer, Acta Metall. 31 (1983) 845.

[39] A. Trayanov and E. Tosatti, in: The Structure of Surfaces II, Eds. J.F. van der Veen, M.A. Van Hove, Vol. II of Springer Series in Surface Science (Springer, Berlin, 1988).

[40] R. Lipowsky, Z. Phys. B 55 (1984) 335, 345.

[41] R. Lipowsky, Phys. Rev. Letters 57 (1986) 2876.

[42] A. Trayanov and E. Tosatti, Phys. Rev. B 38 (1988) 6961.

[43] R. Lipowsky, to be published.

[44] U. Breuer, O. Knauff and H.P. Bonzel, to be published.

[45] J.W.M. Frenken, J.F. van der Veen, R.N. Barnett, U. Landman and C.L. Cleveland, Surface Sci. 172 (1986) 319.

[46] J.C. Heyraud and J.J. Métois, Surface Sci. 128 (1983) 334.

[47] M. Wortis, in: Chemistry and Physics of Solid Surfaces, Vol. VII, Eds. R. Vanselow and R. Howe (Springer, Berlin, 1988) p. 367.

[48] H.P. Bonzel, in: Surface Mobilities on Solid Materials, Ed. Vu Thien Binh (Plenum, New York, 1983) p. 195, and references therein.

[49] G.D.T. Spiller, Phil. Mag. 46 (1982) 535.

[50] H.P. Bonzel, Surface Sci. 21 (1970) 345.

[51] H. Loewen, T. Beier and H. Wagner, to be published.